

**SEISMIC VELOCITY ESTIMATION
USING PRESTACK TIME MIGRATION**

A DISSERTATION
SUBMITTED TO THE DEPARTMENT OF GEOPHYSICS
AND THE COMMITTEE ON GRADUATE STUDIES
OF STANFORD UNIVERSITY
IN PARTIAL FULFILLMENT OF THE REQUIREMENTS
FOR THE DEGREE OF
DOCTOR OF PHILOSOPHY

By
Paul J. Fowler
September 1988

© Copyright 1988
by Paul J. Fowler

printed as Stanford Exploration Project Report No. 58
by permission of the author

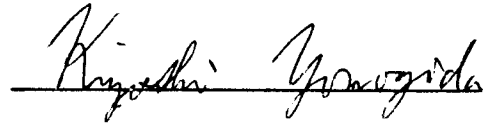
Copying for all internal purposes of the sponsors
of the Stanford Exploration Project is permitted

I certify that I have read this thesis and that in my opinion it is fully adequate, in scope and quality, as a dissertation for the degree of Doctor of Philosophy.

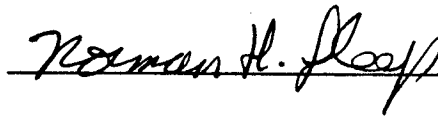


(Principal Advisor)

I certify that I have read this thesis and that in my opinion it is fully adequate, in scope and quality, as a dissertation for the degree of Doctor of Philosophy.



I certify that I have read this thesis and that in my opinion it is fully adequate, in scope and quality, as a dissertation for the degree of Doctor of Philosophy.



Approved for the University Committee
on Graduate Studies:

(Dean of Graduate Studies and Research)

ABSTRACT

Accurate estimation of background velocities is often the most problematic step in imaging seismic reflection data. Conventional methods compute stacking velocities by normal-moveout hyperbolic stacking at a range of velocities, followed by selection of the stacking velocities that correspond to optimal stacks. This method is widely used because it is robust for noisy data. From the stacking velocities an estimate of interval velocities is made, based on assumptions of flat-layered geology and laterally invariant velocity. This estimate degrades in regions with complex geological structure.

A natural extension of conventional velocity analysis replaces normal-moveout stacking by prestack time migration. The assumption of a stratified medium is removed, and the resulting velocity analysis becomes independent of structure. Just as stacking velocities provide the information needed to form a good stacked image, prestack time-migration velocities yield a good time-migrated image. I show here how the processes of dip moveout and migration can be formulated to act on data that is NMO-stacked at a range of velocities, converting a conventional velocity analysis into a prestack time-migration velocity analysis. The resulting algorithm integrates velocity analysis and imaging, enabling practical interactive migration.

For many data, a time-migrated image is sufficient for structural interpretation. Complex geological structure, however, is often accompanied by substantial lateral velocity variation, which necessitates using depth migration for correct imaging. Depth migration requires detailed knowledge of interval velocities. I derive here a linear operator that relates perturbations in interval velocities to the corresponding observed changes in prestack time-migration velocities. This operator formally comprises a filtered version of travel-time tomography, but no picking of traveltimes is required. The resolution possible for long wavelength velocity variations is comparable to that obtained by ray-trace tomographic methods. The linear operator developed here can provide the gradient information required for iterative, nonlinear inversion algorithms. The same linear operator can also be modified for inverting velocities computed from data that is dip-moveout corrected but not migrated. Results from synthetic data suggest that anomalies in the latter type of velocity are easier to measure and invert accurately.

ACKNOWLEDGEMENTS

In working on this thesis I have been privileged to have the counsel of two superb advisors. Jon Claerbout made possible the nonpareil research environment of the Stanford Exploration Project, and provided patient support throughout. Fabio Rocca offered a cornucopia of insights and ideas in the final stages.

I have also been aided by many colleagues along the way. Jeff Thorson started me thinking about velocity spaces, and played midwife to my initial formulation of the concepts of chapter 2. Les Hatton convinced me that velocity analysis was a critical limitation in most imaging; he also facilitated a thoroughly enjoyable summer in Britain, during which time I learned from him many invaluable facts about both seismic data and malt whisky. My work in chapters 3 and 4 builds on that of John Toldi, from whom I have learned much. Others who helped me, principally by means of countless enlightening discussions, include John Sherwood, Francis Muir, Kamal Al-Yahya, John Etgen, Jos van Trier, Dave Hale, Dan Rothman, Helmut Jakubowicz, Bob Shurtleff, Shuki Ronen, Christof Stork, Marta Woodward, Biondo Biondi, Chuck Sword, Bill Harlan, and Peter Mora. Stew Levin and Joe “Pinball Wizard” Dellinger provided many useful suggestions about computer matters as well as geophysics. Pat Bartz and Carol VonderLinden guided me through many a bureaucratic barrier, generously letting me draw upon their reserves of patience and tact on the frequent occasions when my own supplies ran low. David Okaya, Einar Kjartansson, and Jim Scheimer helped me demultiplex the offshore California data and prepare them for further processing. And my fellow inmates on the fourth floor of the Mitchell Building, Jill McCarthy, Erik Goodwin, Bill Harbert, Colleen Barton, and Craig Jarchow, provided vital conversation and camaraderie.

Financial support for this work was provided by a National Science Foundation fellowship and by the sponsors of the Stanford Exploration Project. The Gulf Coast data were donated to SEP by Western Geophysical. The offshore California data were made available by British Petroleum through the kind efforts of Jack Hosken.

I thank all these people and organizations for their generous assistance and friendship; I could not have done this work alone, and I am indebted to them all.

Table of Contents

Abstract	v
Acknowledgments	vii
List of figures	xi
Chapter 1: Introduction and overview	
1.1 Velocity analysis for reflection seismology	1
1.2 Stacking velocity analysis	5
1.3 Reflection tomography	7
1.4 Velocity analysis using prestack migration	8
1.5 Assumptions and limitations	10
Chapter 2: Dip moveout and migration in velocity space	
2.1 Introduction	13
2.2 Imaging in velocity space	15
2.3 Allowing for spatially varying velocity	23
2.4 Field data examples	27
2.5 Velocity analysis using velocity-space imaging	37
2.6 Sampling velocity space	48
2.7 Velocity-space imaging for three-dimensional data	54
2.8 Conclusions	66
Chapter 3: A linear operator relating interval and migration velocities	
3.1 Introduction	67
3.2 A linear operator	68
3.3 Filtered tomography	69
3.4 Computing the general operator	72
3.5 Weighting dips selectively: the dip-dependent operator	77
3.6 The linear operator for constant slowness background	81
3.7 A degenerate degree of freedom	84
3.8 The flat-dip operator	85
3.9 Visualizing the operator	89
3.10 Conclusions	105
Chapter 4: Predicting and inverting migration velocities	
4.1 Introduction	109
4.2 Predicting the effects of slowness anomalies	109
4.3 Inverting the linear operator	120
4.4 Improving (and degrading) resolution	136
4.5 Formulating nonlinear inversion	151

4.6 Discussion and conclusions	158
Appendices	
Appendix A: The equivalence of velocity-space DMO and Hale's DMO	161
Appendix B: Computing the effective offset ratio γ at zero offset	165
Appendix C: Decomposing the travelt ime pyramid into dip components	167
Appendix D: Comparing two methods for least-squares fitting of hyperbolas ..	171
Appendix E: An alternative algorithm for nonlinear inversion	175
Appendix F: The movement of reflectors during migration	179
References	183

List of Figures

1.1	Example of imaged seismic reflection data	2
1.2	Example of seismic reflection field data	3
1.3	Velocity field used for migrating data in Figure 1.1	4
2.1	Synthetic zero-offset data compared with velocity-space DMO processing	17
2.2	Low and high velocity stacks of synthetic data	18
2.3	Velocity-space imaging compared with prestack Stolt migration	20
2.4	Interpolating a variable velocity image by slicing a velocity cube	24
2.5	Synthetic data and velocity-space DMO for $v(z)$	25
2.6	Velocity-space DMO and migration for $v(z)$	26
2.7	Gulf coast stacked section	28
2.8	Gulf coast section after velocity-space DMO	29
2.9	Gulf coast section after velocity-space DMO and migration	30
2.10	Low and high velocity stacks of a window from the Gulf coast data	31
2.11	Low velocity stack from Figure 2.10 after DMO and migration	32
2.12	Velocity function for processing Gulf Coast data	33
2.13	Offshore California stacked section	34
2.14	Offshore California section after velocity-space DMO	35
2.15	Offshore California section after velocity-space DMO and migration	36
2.16	Stacking velocity function for offshore California data	37
2.17	Migration velocity function for offshore California data	38
2.18	Velocity analysis at one midpoint from Figure 2.7	39
2.19	Velocity analysis of Figure 2.14 after DMO	40
2.20	Velocity analysis of Figure 2.14 after DMO and migration	41
2.21	Velocity analyses for $v(z)$ synthetic data	42
2.22	Window of offshore California data imaged with various velocities	46
2.23	Window of offshore California data imaged with various velocities	47
2.24	Window of offshore California data imaged with various velocities	49
2.25	Window of offshore California data imaged with various velocities	50
2.26	Conventional NMO stack of the Gulf coast data	55
2.27	Difference between Figures 2.7 and 2.26	56
2.28	Velocity-space stack using twice as many stacks as Figure 2.7	57
2.29	Difference between Figures 2.7 and 2.28	58
2.30	Velocity-space stack using half as many stacks as Figure 2.7	59
2.31	Difference between Figures 2.7 and 2.30	60
2.32	Velocity-space migration using half as many stacks as Figure 2.9	61
2.33	Difference between Figures 2.9 and 2.32	62
2.34	Geometry of 3-D dip-moveout	64

3.1	Traveltime pyramid for a point diffractor in prestack data	71
3.2	Geometry of rays for a single diffracting point	74
3.3	Geometry of rays for a dipping bed: CRP and CMP	79
3.4	Traveltime pyramid showing dip decomposition	80
3.5	Geometry of rays for a dipping bed in a constant velocity medium	82
3.6	\mathbf{G}_s operator for reflecting point on a flat bed	90
3.7	Effects of traveltime perturbations on moveout hyperbolas	91
3.8	\mathbf{G}_r operator for reflecting point on a flat bed	92
3.9	\mathbf{G}_s operator for reflecting point on a dipping bed	93
3.10	Cross sections through the \mathbf{G}_s operator of Figure 3.9	94
3.11	\mathbf{G}_r operator for reflecting point on a dipping bed	96
3.12	\mathbf{G}_y operator for reflecting point on a dipping bed	97
3.13	\mathbf{G}_s for a fixed anomaly point and flat beds	98
3.14	Cross sections through the \mathbf{G}_s operator of Figure 3.13	99
3.15	\mathbf{G}_s for a fixed anomaly point and dipping beds	100
3.16	Cross sections through the \mathbf{G}_s operator of Figure 3.15	101
3.17	\mathbf{G}_s operator for cable with non-zero inner offset	103
3.18	\mathbf{G}_s operator for depth-variable background slowness	104
3.19	Dmo slowness operator for a fixed anomaly point and flat beds	106
3.20	Dmo slowness operator for a fixed anomaly point and dipping beds	107
4.1	Slowness model: flat bed, Gaussian anomaly, and constant background	111
4.2	Finite-difference synthetic data for slowness model of Figure 4.1	112
4.3	Predicted versus measured migration slownesses for model of Figure 4.1	112
4.4	Slowness model: dipping bed, Gaussian anomaly, and constant background	113
4.5	Finite-difference synthetic data for slowness model of Figure 4.4	114
4.6	Measured stacking slownesses for model of Figure 4.4	114
4.7	Predicted migration slownesses for model of Figure 4.4	115
4.8	Measured migration slownesses for model of Figure 4.4	115
4.9	Horizon slowness analysis for dipping bed of Figure 4.4	116
4.10	Predicted migration slownesses for migrated midpoints in Figure 4.4	117
4.11	Skew-corrected horizon slowness analysis for Figure 4.4	118
4.12	Uniform background migration horizon slowness analysis for Figure 4.4	119
4.13	Predicted versus measured migration slownesses for model of Figure 4.4	120
4.14	Predicted versus measured DMO slownesses for model of Figure 4.4	121
4.15	Inversion of \mathbf{G}_s operator for flat bed model of Figure 4.1	123
4.16	Example of \mathbf{G}_s operator used in Figure 4.15	124
4.17	Inversion of \mathbf{G}_s operator with artifacts lessened	125
4.18	Singular value spectrum of \mathbf{G}_s operator for inversion of Figure 4.17	126
4.19	Selected model-space singular vectors for inversion of Figure 4.17	127
4.20	More model-space singular vectors for inversion of Figure 4.17	128
4.21	Inversion of \mathbf{G}_s operator for dipping bed model of Figure 4.4	130
4.22	Singular value spectrum of \mathbf{G}_s operator for inversion of Figure 4.21	131
4.23	Selected model-space singular vectors for inversion of Figure 4.21	132
4.24	More model-space singular vectors for inversion of Figure 4.21	133
4.25	Traveltime tomographic inversion of dipping bed model of Figure 4.4	134

4.26	Inversion of DMO slowness operator for dipping bed model of Figure 4.4	... 135
4.27	Inversion of measured migration slownesses for dipping bed of Figure 4.4	... 137
4.28	Inversion of \mathbf{G}_s operator for Figure 4.4 using short cable 138
4.29	Inversion of measured DMO slownesses for dipping bed of Figure 4.4 139
4.30	Inversion of \mathbf{G}_s operator for 3 parallel dipping beds 140
4.31	Inversion of \mathbf{G}_s operator for 3 non-parallel dipping beds 141
4.32	Predicted migration slownesses using different offset ranges 142
4.33	Inversion of \mathbf{G}_s operator using outer offsets only 143
4.34	Joint inversion of \mathbf{G}_s operator using inner and outer offsets 144
4.35	Predicted traveltimes pullup for flat bed model of Figure 4.1 145
4.36	Inversion of \mathbf{G}_r operator for flat bed model of Figure 4.1 147
4.37	Singular value spectrum of \mathbf{G}_r operator for inversion of Figure 4.36 148
4.38	Selected model-space singular vectors for inversion of Figure 4.36 149
4.39	Joint inversion of \mathbf{G}_s and \mathbf{G}_r for flat bed model 150
4.40	Inversion of \mathbf{G}_s operator for a segmented reflector 152
4.41	Inversion of \mathbf{G}_s operator for a severely segmented reflector 153